AMSE Association for the Advancement of Modelling & Simulation Techniques in Enterprises
IIETA International Information and Engineering Technology Association
Advancing the World of Information and Engineering

Modelling, Measurement and Control C
Vol. 79, No. 2, June, 2018, pp. 46-55
Journal homepage: http://iieta.org/Journals/MMC/MMC_C

Development of a universal blast-induced ground vibration prediction model for Jharia coalfields

Dayamoy Garai[1], Arvind Kumar Mishra[2], Shankar Kumar[2], Hemant Agrawal[3*]

[1] Central mine planning and design institute limited, Ranchi 834008, India
[2] Indian Institute of Technology (ISM), Dhanbad, 826004, Jharkhand, India
[3] Deputy Manager, Coal India Limited, India

Corresponding Author Email: hemant.ism@gmail.com

https://doi.org/10.18280/mmc_c.790205

Received: 13 May 2018
Accepted: 20 June 2018

Keywords:
ground vibration, random forest, artificial neural network, coal mines, scaled distance

ABSTRACT

Mineral commodities are the backbone of every nation as they contribute to the Gross domestic product (GDP), industries (as raw materials), and foreign exchange. Coal production in India is 724.71 MT (Million Tonnes) in year 2015. The production target has been increased by the government of India to 1.5 billion tonnes by 2022. Opencast mining in 2015 contributed to 639.234 MT (88%) of total coal production in India. This increased demand of coal shall compel the mine owner to operate under greater stress to increase the production rate. So, there will be situations arising that the mine owners may have to extract coal near human habitats. Eight of the major mines were selected and necessary care was taken that all the geological areas occurring in the Jharia coalfield region was covered. Various blast design parameters such burden, hole depth, spacing, charge per delay(CPD), and scaled distance were selected for the study of ground vibration. Data mining methods such as random forest and artificial neural networks(ANN) has been used for the prediction of peak particle velocity(PPV). The model formed by the two methods was compared and validated by selecting another two mines. The results obtained by random forest was superior to ANN. Also, a line at 95% confidence interval for the predicted PPV values is drawn to ensure greater safety. With 95% confidence and universal blast induced ground vibration prediction model for jharia coalfield has been developed. This model will help the blasting engineers operating in jharia coalfields in precise prediction and better control over blast induced ground vibration. The concept of this study can be used for generation of blast induced ground vibration prediction models for different coalfields also.

1. INTRODUCTION

Minerals play an important role in the growth of a nation. The demand for the minerals is increasing rapidly in the world. To cope up with the growing demands of the minerals large-scale mines are being planned. Though the advancement of rock cutting machinery has taken place still applicability to various geology is not known and rate of production is lower than drilling and blasting and it is also costly. Blasting performance is directly related to the characteristics and efficiency of the explosives used [1]. Blasting requires large amount of explosive and proper blast design for efficient results. Blasting is economical and applicable in almost all the geological conditions but it has many disadvantages too. Only 25–30% of the explosive energy is utilized for breaking and displacement of rocks [2] and rest of the energy creates nuisance. The negative hazards of blasting are air blast, ground vibration, noise backbreak, overbreak, endbreak and flyrock. The major activities which contribute to ground vibration are blasting, movement of machinery. These hazards can affect the structures nearby and also cause a disturbance in the water table and wells and dwellings nearby. It may also cause fear, and annoyance, and may lead to complaints, work delays and legal processing by the people staying in the nearby. Human beings response to vibration levels at much lower than the levels established as Structural damage thresholds [3].The magnitude of ground and structure vibrations caused by blasting depends on the blasting methods, soil and rock medium, heterogeneity of soil and rock deposit at the site, distance from the source, characteristics of wave propagation at a site, dynamic characteristics of soil and rocks, response characteristics of fractures and susceptibility rating of the structures [4]. Ground vibrations factors that determine the degree of house shaking are ground vibration amplitude (peak particle velocity), its duration and its dominant frequency and the response frequencies of the structure [5]. One of the major problem in blasting is to eliminate ground vibration [6-7]. In India DGMS have issued circular No. 7 in 1997 for ground vibration levels.

It has been inferred from literature that peak particle velocity (PPV) is generally a good index of damage to structure. Blast-induced ground vibrations are characterized by two important parameters, i.e. the peak particle velocity (PPV) and frequency. The relationship between PPV and scaled distance (D) can be written as

$$v = kD^b$$

where,
v = PPV (m/s);
D = Scaled distance ($m/\sqrt{kg}$)
k and b = Site constants.

Scaled distance which is defined as the ratio of distance

from charge point, R (m), to the square root of charge per delay, Q (kg).

Due to the rising human population which has led to the expansion of human habitats and come near to the vicinity of operating mines. The demand for minerals has also increased rapidly with time. So, we have to increase our production without compromising safety. Due to the stringent environmental protection laws and growing awareness among the people causes confrontaion between local residents and mine management. This causes lock downs and increases the lock in period of minerals. Sometimes the mining activity is stopped which causes great loss to the nation as the mineral resources remain locked. Many researchers have come up with empirical methods and machine learning tools to predict ground vibration. ANN is a machine learning tool which has been used to predict ground vibration so that they can overcome the limitations of empirical equations [8-12]. Genetic algorithm [13], Random forest [14] and support vector machines [14-15] have also been in trends to predict ground vibration by various researchers. Statistical tools, such as multivariate regression analysis [1, 9] is also used to predict ground vibration.

1.1 Ground vibration

Ground vibration consideration is gaining significance with decreasing level of people tolerance of vibration, introduction of new environmental legislation, increasing use of equipment sensitive to vibration, ageing of existing buildings and expanding construction sites. Vibration consideration involves its source, propagation path and its recipient. The intensity of ground vibration depends on various parameters which can be divided into two classes controllable and non-controllable parameters. Ground vibrations are the technical term for describing the vibrations caused by the man-made activities. Wave parameters are the properties used to describe the wave motion such as amplitude, period, crest, trough and frequency. Vibration parameters are the physical quantities used to describe vibration. These are displacement, velocity, acceleration and frequency. A seismograph system measures three mutually perpendicular components of ground motion designated vertical, longitudinal and transverse.

Ground vibrations are composed of mainly two types of waves known as body waves and surface waves. The name body waves are given as they propagate through the rock and surface waves travel at the surface of the rock as they do not penetrate through the rock.

The body waves can be further classified into two categories that is P wave and S wave. Rayleigh wave generated by the interaction of P- and S-waves at the ground surface is termed as the surface wave [16]. It should be noted that S-wave component plays an important role in damage to rock or adjacent structures [17], and it might induce considerable amplitude of vibration in specific directions compared to P-wave.

The transmitting of vibration energy occurs because ground tends to reach the state of a minimum energy when disturbed by vibration [18]. Ground disturbance by a vibration source causes occurrence of stress waves, which transmit the source energy in the form of energy flux. The total energy-flux density Eflux per unit time (i.e. wave power) in direction of wave propagation through wavefront area dS is in the case of an isotropic stress-strain relationship in a non-dispersive (closed) system [19].

2. EXPERIMENTAL SITES

In Jharia coalfields many of the mines are located near to the human habitat and other sensitive structures. There are situations arising often that there is a face off between the mine management and the local peoples. This often leads to losses as it stops the work of the mines. So to avoid this situations in future there was a need to develop a model or formula to get the safe distance for blasting. So for this study 8 of the major coalmines located in the Jharia coalfields were selected for the study and model preparation using ANN and random forest. The models formed were than validated by selecting another two mines from the Jharia coalfield. Blast design parameters such as burden, spacing, hole depth, CPD and scaled distance were selected for the study. PPV of the selected mines were monitored in the field with vibrometer.

2.1 Mine details

Mine 1

The mine is located between a latitude $23^0$43’24’’ north to 23043’48’’ and longitude 85034’33’’ east to 85034’40’’ at a distance of about 17 KM from the Sub Regional office this Directorate at Ramgarh. Hazaribag and Ranchi is about 35KM and 60KM respectively. The mine lies in the north dipping southern flank of the southern sub-basin of the west Bokaro Coalfield and its leasehold area. Presently five coal seams i.e. seam III, IV, V, VA, VI are being worked under Mine 1. The overburden comprises of hard to medium hard sandstone.

Mine 2

The major part of the area is under soil cover. Rocks of Barakar Formation lie below the soil cover and are exposed in patches in the northern and north-western part. These rocks are having faulted contact with the rocks of Barren Measure Formation in southern part of the area.

(I) Strike and Dip: The strike of the seam is generally trending NE-SW in the western part, E-W in the central part and swings to NW-SE in the eastern part. The dip is generally southerly trending and ranges from 4^0 in the central part to about 7^0 in the western corner of the project area.

(II) Faults: Three major faults are encountered in the area. The throw of these faults varies up to 240m.

Mine 3

The Mine C is located in the eastern-central part of Jharia Coalfield in Dhanbad district of Jharkhand. The Mine ‘C’ lies between latitude 23o 42’14” to 23˚43’59”N and longitude 86˚24’43” to 86° 26' 45"E. The area is covered under Topo sheet No- 73-I/6. The mine area is covered by various types of rocks belonging to Barakar Formation of Lower Gondwana group under a moderately thick cover of soil, alluvium and sandy soil. The major portion of the cluster is covered by alluvium and sandy soil of recent age,which range in thickness from 1.6 m to 1.8 m and occupy lower grounds.Metamorphic rocks cap the higher grounds, mainly in the northern part of the block.The thickness of the top formation up to weathered mantle varies from 0 to 11.60 m,made up of alluvium, sandy soil with consolidated weathered Barakar sandstone and is underlain by the coal-bearing rocks of Barakar Formation. Barakar formation, occurring below the soil covers, consists of sandstone,argillaceous sandstone, arenaceous shale, carbonaceous shale, grey shale and coal seams.

Mine 4

Mine 4, located in BCCL. All the seams are presently being excavated by Surface miner. Three surface miners have been

deployed in the project for winning the coal .However, some portions of the coal seam left by the surface miners is being excavated through conventional blasting. The gradient of the seams is 1 in 20.Transportation of coal is being done by pay loader – tipper combination.

Mine 5

The basic structure of the concerned block is simple. The general strike in the area is almost north-south. The average dip varies from 5º to 10º towards west. There are four coal seams occurring in the concerned blocks, viz. Kota, Turra, Purewa bottom and Purewa Top seams in ascending order. The bottom-most seam (Kota seam) has been encountered only in few boreholes. It occurs 68 to 100m below Turra Seam. The thickness of the Seam varies from 2.2 to 3.0m (including dirt bands). Kota seam is currently not being considered for mining.

Mine 6

The Mine 6 Opencast project falls within Halong and South geological blocks. It is located in the south central part of North Karanpura Coalfields and is included in Survey of India toposheet no. 73 E/2 and 73 A/14 in Ranchi district of Jharkhand. The coal bearing rocks and the coal seams occurring within the mine area belong to the Barakar Formation of the Lower Gondwana Group. The contact between the coal bearing rocks and metamorphics in the South is faulted. The general strike of the beds in the part of Karkata block, is in WNW-ESE. The gradient varies from 1 in 9 to 1 in 4 due South.

Mine 7

Mine 7 Open Cast Project is located over Kulda Block of-of IB valley Coalfield. In Mine 7 Block, Rampur seam, and Lajkura seam occurs in the Barakar formations and IB seam occurs in Karharbari formation of Lower Permian Age. Strike of the Strata is roughly NW-SE. The dip is generally 7º towards southwest. Dip is slightly higher in southern part and near faults compared rest of the area. There are three coal seams viz. Ib, Rampur & Lajkura. Ib is the bottom most coal seams and spat into three sections viz. Ib Top, Ib Middle & Ib Bottom. Rampur seam is splitted into five sections namely Rampur-I, Rampur-II, Rampur-III Top, Rampur-III Bottom, Rampur –IV& Rampur-V. Lajkura is also a thick seam and splitted into four sections viz.Lajkura-I, Lajkura-II, Lajkura-III & Lajkura-IV.

Mine 8

Almost entire block has been covered by Barakar formations containing five main coal seams which are designated as seam – I to seam – V in ascending order. The strike of the formations in the Magadh block are NE-SW which swings to ENE-WSW in the eastern part. The dip of the formations generally varies from 4^0 to 9^0 towards south. Magadh block has been intersected by two faults (F1 & F2). The fault F1 forms the eastern boundary of the Magadh block is a major fault trending WNW-ESE having maximum throw of 120 m the other fault F2 is a small oblique fault trending NNE-SSW having a throw of 7 m towards west.

2.1.1 Mine location

The figure 1 shows the details of all the mines selected for this study. After the study the two site constants were found out. It also shows the mines A,B where after the study the trial blasting is carried out.

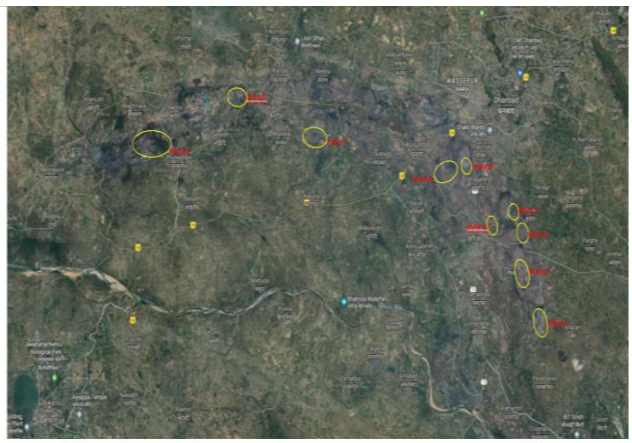

Figure 1. Location of selected mines in Jharia coalfield for development of model

2.2 Data collection

Parameters like burden spacing and hole depth are the characteristic property of the mine that needs to be taken as practised values in the mine. The charge per delay of the blast was also taken into consideration as an input parameter as it plays a important role in generation of ground vibration. The measurement point where the instrument was kept for monitoring is taken as distance as one of the input parameters. The details of compressive strength has been obtained by using N-type Schmidt hammer value Based on this the strata was divided into four classes like from soft medium hard and very hard into 0.25 0.5 0.75 and 1.0. The classification of the strata was done by calculating the uniaxial compressive strength of the strata as shown in the table 1.

Table 1. Schmidt hammer rebound index and compressive strength of rocks encountered

Serial no.	Schimdt hammer rebound index	Compressive strength(Mpa)	Class	Value assigned
1	47-56	>50	Very hard	1
2	36-46	40	Hard	0.75
3	29-35	30	Medium hard	0.5
4	23-28	20	Soft	0.25

Table 2. Range of input and output parameters

Parameter	Unit	Symbol	Description	Range	Mean	Standard deviation
Hole depth	M	D	Input	3 – 7	5.638	0.654
Burden	M	B	Input	2 – 5	3.549	0.525
Spacing	M	S	Input	2.5 – 6	4.389	0.689
Charge Per delay	kg/m^3	Q	Input	15.1 – 80.2	48.029	12.105
Distance	M	D	input	45 – 950	206.754	171.727
Peak particle velocity	mm/s	P	Output	0.5 – 33.84	6.689	5.519

2.3 Determination of interdependence of input parameters

2.3.1 Covariance

Covariance is a measure of how changes in one variable are associated with changes in another variable. Specifically, covariance measures the degree to which two variables are linearly associated. However, it is also often used informally as a general measure of how monotonically related two variables are. The covariance of depth, burden, spacing, CPD, distance and PPV was determined using Excel software of Microsoft office.

Table 3. Covariance of parameters

	Depth	*Burden*	*Spacing*	*CPD*	*Distance*	*PPV*
Depth	0.426696					
Burden	0.249559	0.274429				
Spacing	0.352571	0.344026	0.472872			
CPD	6.875815	4.432095	6.935198	146.0217		
Distance	18.5394	26.14715	33.22899	535.8109	29386.75	
PPV	0.409493	0.244808	0.464917	7.901487	-484.16	30.35759

The table 4 indicates that the stated parameters are having significant influence on blast induced ground vibration.

2.3.2 Correlation

Correlation is a statistical measure that indicates the extent to which two or more variables fluctuate together. A positive correlation indicates the extent to which those variables increase or decrease in parallel; a negative correlation indicates the extent to which one variable increases as the other decreases. The correlation of depth, burden, spacing, CPD, distance and PPV was determined using Excel software of Microsoft office.

Table 4. Correlation of variables

	Depth	*Burden*	*Spacing*	*CPD*	*Distance*	*PPV*
Depth	1					
Burden	0.729289	1				
Spacing	0.784902	0.955002	1			
CPD	0.871077	0.700141	0.8346	1		
Distance	0.165562	0.291161	0.281884	0.258659	1	
PPV	0.113777	0.084816	0.122707	0.118677	-0.5126	1

Negative value relation between the distance and the PPV shows that it is inversely proportional. As we move further from the blasting site the high frequency waves attenuates and loses its strength. Positive values indicate that they are directly proportional to each other.

2.3.3 Analysis of variance (ANOVA)

Analysis of variables (ANOVA) was obtained for the parameters depth, burden, spacing, CPD, distance and PPV by using Excel software of Microsoft office.

Table 5. ANOVA table

Source of Variation	SS(Sum of Squares)	Df (Degrees of freedom)	MS(Mean sum of squares)	F (F-statistics)	P-value	$F_{stastics}$
Between Groups	9277869	5	1855574	375.2627	1.33E-271	2.219349
Within Groups	8425825	1704	4944.733			
Total	17703694	1709				

The P value obtained in the table is small as there has been random sampling of data from 8 different mines using different blast design patterns.

3. WORKING STEPS OF RANDOM FOREST

The random forest algorithm uses a standard machine learning technique known as “decision tree”. Input is entered at the top in the decision tree and as it travels below the tree the data gets grouped into smaller and smaller groups. In this manner all the data set moves below the tree and its relationship will be calculated for each stage. If two stages come at same point their nearness will be increased by one. At the last implementation stage the relationship are normalized by dividing the number of trees [20]. These relationships help in substituting missing data finding out outliers. The random forest tree has subsequent working step to training a system Sample N cases at random with replacement to create a subset of the data. This subset of data should be about 85% of the total dataset.

1. At each node, for some m- number, m predictor variables are chosen at random from all the predictor variables. The predictor variable provides the best split, according to some objective function. The binary split will be taking place on that node.
2. At the next node, choose another m variables at random from all predictor variables and repeat it as same.
3. Depending upon the value of m, there are three slightly different systems
    1. Random splitter selection: m=1
    2. Breiman’s bagger: m = total number of predictor

variables

3. Random forest: m << number of predictor variables. Brieman suggests three possible values for m: ½√m, √m, and 2√m

Random decision forests correct for decision trees habit of overfitting to their training set, and final prediction can simply be the mean of each prediction [21].

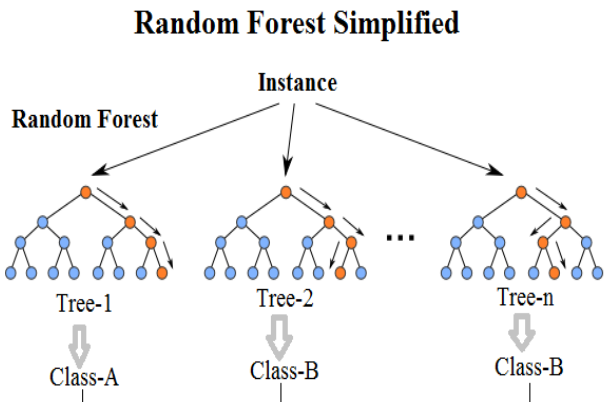

Figure 2. Schematic diagram showing the information flow in random Forest algorithm

In the present study a total of 285 blast data was considered. The data available was divded into two parts one was training datset and other was testing dataset. Training dataset consisted of 85% of the data and was used to train the data set and the remaining 15% data was used as test dataset and their values were predicted by the model formed which was compared with actual results obtained on the ground for variation.

3.1 Network architecture

The prediction of ground vibration has been monitored and documented with a set of 285 data set points. These data set is examined and categorised employing random forest algorithm with k fold crossover validation to verify the regularity and grade of the data. The classifier eventually divided into training data set to train the model and testing data set to judge the prediction model. The original data sample is randomly divided into k equal subparts With k subsamples a single part of data is kept as the validation data for testing the model while remaining k 1 parts are used as training purpose for the model. This crossover validation procedure is then carried out k times where each k subparts of data used exactly once as the validation data. The k results from the folds can then average to produce a single predicted value. In this study we have implemented 10 fold crossover validation for prediction of blasting data. With different coefficient of determination such as correct classified accuracy, incorrect classified accuracy, mean absolute error and mean square errors. The output results clearly show that the random forest-based model has the magnitude to predict the peak particle velocity shown in table 6.

Table 6. Analysis result by random forest

Serial no.	Methods	Values
1	Correlation coefficient	0.9836
2	Kendall's tau	0.7794
3	Spearman's rho	0.9187
4	Mean absolute error	0.7464

Table 7. Predictions of PPV made by random forest

Serial No.	Actual	Predicted	Error
1	3.422	3.0652	-0.819
2	0.641	1.0743	-0.324
3	4.58	2.9011	1.05
4	4.839	3.3094	-0.006
5	2.53	3.1528	-0.063
6	3.297	3.6182	-0.277
7	5.842	5.7608	-0.529
8	4.529	5.196	-0.493
9	3.854	4.2895	-1.053
10	7.94	8.7782	0.186
11	3.234	1.7498	-2.201
12	6.507	6.3485	0.829
13	4.202	3.8522	0.155
14	1.428	1.60275	-2.527
15	2.08	1.8445	0.152
16	4.223	3.5071	-0.77
17	19.72	18.7092	7.435
18	4.328	3.2826	0.022
19	2.66	3.6745	-0.343
20	4.943	5.2636	-0.573
21	2.812	3.7337	-1.46
22	5.841	6.234	0.671
23	4.07	3.9126	1.092
24	26.5	24	1.117
25	9.095	11.8842	-0.56
26	8.071	9.034	0.197
27	5.182	5.5794	0.056
28	3.694	4.6068	-0.054
29	6.706	7.5934	-1.183
30	2.31	1.9301	0.22
31	7.972	7.5934	0.075
32	2.658	2.906	-0.023
33	2.36	3.1826	0.531
34	2.843	2.0203	0.021
35	7.14	6.4485	0.78
36	4.982	3.1528	0.087
37	2.768	2.6558	0.175
38	2.306	2.2106	-0.008
39	2.93	4.9436	1.595
40	5.102	3.8376	-0.365
41	2.693	4.7906	-0.25
42	5.015	6.0201	-1.182
43	6.944	6.501	0.584

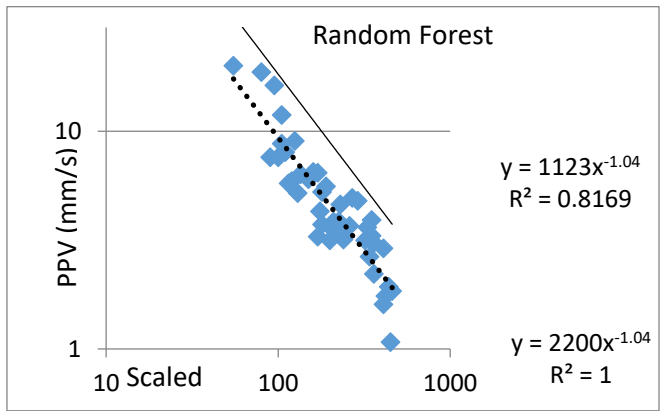

Figure 3. Graph between predicted PPV by random forest and scaled distance

Figure 3 shows relation between the scaled distance and predicted PPV by random forest method. Series 1 represents the best fit curve on the predicted values with R^2 value of 0.82

while series 2 is the 95% prediction curve for PPV prediction with 95% confidence interval.

3.3 Artificial Neural Network (ANN)

Muhammad & Shah (2017) used ANN to control backbreak in limestone mines [22]. Raymond (2016) successfully used ANN to predict blast induced ground vibration [9]. Khandelwal & Singh (2009), used and successfully applied the neural network method in the field of blasting and waste dump stability [2]. The blast vibration was monitored and documented into 285 blast dataset. This data was divided into three parts eventually training dataset (70%), validation dataset (15%) and test dataset (15%). The complete structure and architecture of the network are illustrated in a flowchart as shown in figure 4.

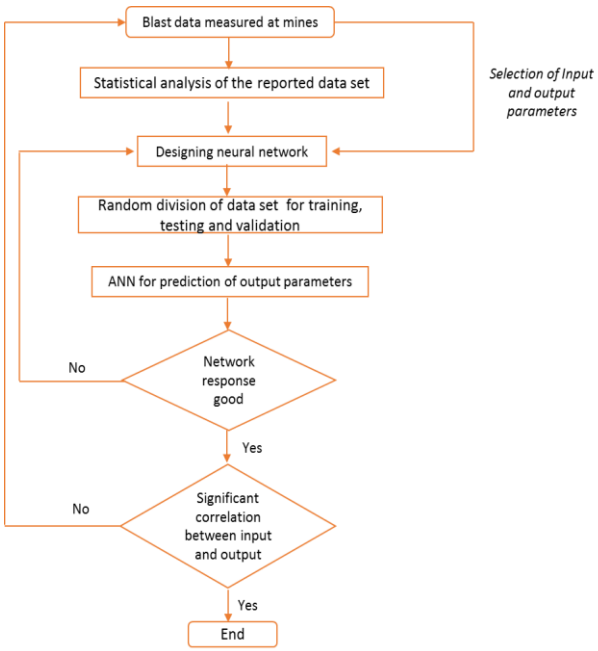

Figure 4. Architecture of ANN process

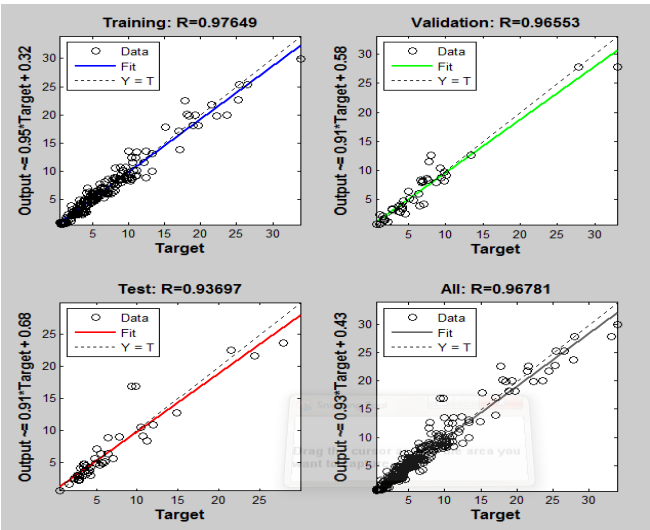

Figure 5. Showing the regression coefficients during training testing and validation

3.3.1 Network training

The training algorithm of the neural network is necessary to interpret the results of the network which include initialization of weights, back-propagation errors and updating weights and biases [23].

Levenberg – Marquadart training algorithm has been used in the present study to train the network. The method is the fastest method for training with high accuracy and convergence speed (MathWorksInc). The behaviour of the network depends on both transfer functions and weights assigned. There are 3 transfer functions considered i.e. Log-Sigmoid, Tan-Sigmoid and Purelin function (Fig. 7). The output of transfer function is passed to the output layer, where it is multiplied by the connection by the connection weights between the output layer and hidden layer. Fig. 8 demonstrate the structure of back propagation neural network with 1 hidden layer and Fig. 9 represents the regression plots of ANN during training, testing, and validation process.

3.3.2 Network validation

The test and validation data set were used to validate the designed network. The weight and biases have been obtained using training data. After training process, measurement of the accuracy of 120 data sets, were simulated to, reach final outputs and check the accuracy of the model. Validation of the model is required to show that the build model is performing non-linear analysis properly or not. An R-squared value between inputs and output and RMSE were used to check the performance of ANN models. The results of ANN models (Table 2) shows different coefficient of determination and mean square errors. The results clearly indicate that the ANN model has the capacity to predict the blast design parameters considered as output, very close to measured values and that the accuracy is acceptable.

Table 8. Summary of predicted values of PPV for Mine A

Serial No.	PPV	RF	ANN
1	10.9	12.32	7.645
2	9.631	7.957	11.142
3	5.709	6.354	7.257
4	4.879	4.989	3.124
5	12.73	11.287	14.587
6	12.98	10.021	15.987
7	3.334	4.178	1.549
8	2.968	3.456	4.12
9	4.155	1.987	3.974
10	4.156	5.248	3.543
11	4.229	5.503	6.55
12	4.704	5.978	7.025
13	7.304	8.578	9.625
14	5.851	7.125	8.172
15	6.438	7.712	8.759
16	7.131	8.405	9.452
17	15.72	16.994	18.041
18	15.85	17.124	18.171
19	6.614	7.888	8.935
20	6.664	7.938	8.985

Figure 6 shows relation between the scaled distance and predicted PPV by random forest method. Series 1 represents the best fit curve on the predicted values with R^2 value of 0.75 while series 2 is the 95% prediction curve for PPV prediction with 95% confidence interval.

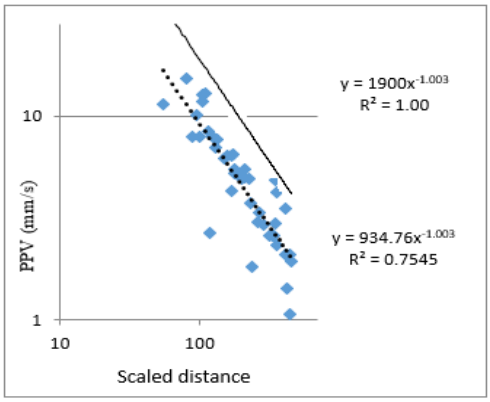

Figure 6. Graph between the predicted values by ANN and the scaled distance

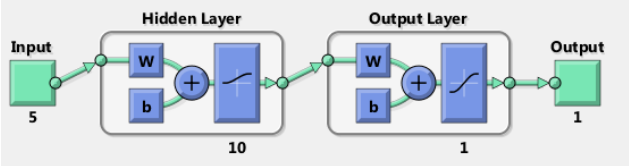

Figure 7. Structure of back propagation neural network

4. ANALYSIS OF RESULTS

The results obtained by both the methods are in acceptable range in most of the cases as it is close to the actual value obtained on the ground. The predicted values obtained by the ranodom forest is found to be more closer to the actual value compared to the ANN. Therefore the random forest method is found to be more encouraging in prediction as compared to the ANN. These prediction methods will help the blast engineers to input different blast design combinations and to predict the PPV values in advance while conducting the controlled blasting near the habitation or structures. This will help in selecting the most suitable blast design in which the predicted PPV values will be minimum. Further to validate the developed model of random forest and ANN total of two mines A & B is selected from the Jharia coalfield and total of 40 blasts were conducted. The PPV was predicted using random forest and ANN while actual PPV was monitored in the mines. The two site constants were obtained by both the methods from the graph. With the help of the two models the vibration levels of Mine A & B were predicted and were compared with actual ground results. The sample of the data comparisons is presented below in the table 8 and 9 respectively.

Table 9. Summary of predicted values by ANN

Serial No.	Actual	Predicted	Error
1	3.422	4.241	0.3568
2	0.641	0.965	-0.4333
3	4.58	3.53	1.6789
4	4.839	4.845	1.5296
5	2.53	2.593	-0.6228
6	3.297	3.574	-0.3212
7	5.842	6.371	0.0812
8	4.529	5.022	-0.667
9	3.854	4.907	-0.4355
10	7.94	7.754	-0.8382
11	3.234	5.435	1.4842
12	6.507	5.678	0.1585
13	4.202	4.047	0.3498
14	1.428	3.955	0.82525
15	2.08	1.928	0.2355
16	4.223	4.993	0.7159
17	19.72	12.29	1.0108
18	4.328	4.306	1.0454
19	2.66	3.003	-1.0145
20	4.943	5.516	-0.3206
21	2.812	4.272	1.0783
22	5.841	5.17	-27.933
23	4.07	2.978	0.1574
24	26.5	25.38	21.7732
25	9.095	9.655	-1.7892
26	8.071	7.874	-0.6283
27	5.182	5.126	-0.3974
28	3.694	3.748	-0.9128
29	6.706	7.889	-0.8874
30	2.31	2.09	0.3799
31	7.972	7.897	0.3786
32	2.658	2.681	0.7279
33	2.36	1.829	-0.8226
34	2.843	2.822	-3.1773
35	7.14	6.36	2.6915
36	4.982	4.895	1.8292
37	2.768	2.593	0.1122
38	2.306	2.314	0.0954
39	2.93	1.335	-2.0136
40	5.102	5.467	1.2644
41	2.693	2.943	-2.0976
42	5.015	6.197	-1.0051
43	6.944	6.36	0.443

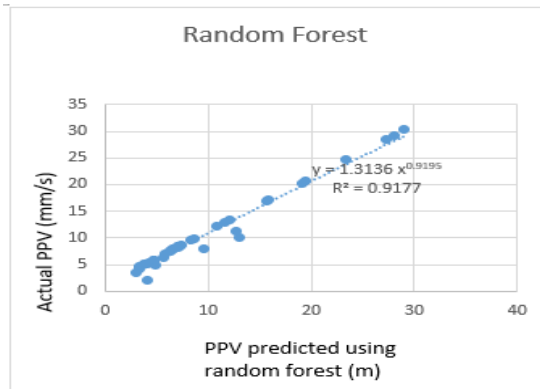

Figure 8. Graph between actual and predicted PPV values by random forest

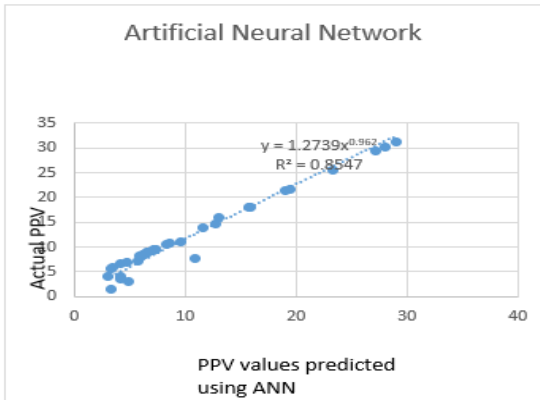

Figure 9. Graph between actual PPV values and predicted PPV values by artificial neural network

Figure 8 is the graph between actual PPV and predicted PPV values by Artificial Neural Network with R^2 value of 0.8547 shows they are in consonance with each other.

Figure 9 is the graph between actual PPV and predicted PPV values by Artificial Neural Network with R^2 value of 0.8547 shows they are in consonance with each other.

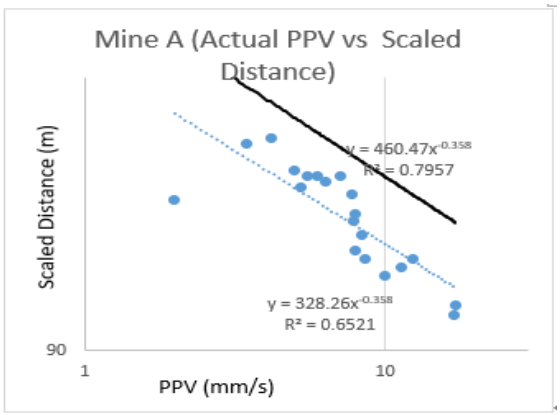

Figure 10. Graph between actual values of PPV for mine A Vs scaled distance

Figure 10 shows relation between the scaled distance and actual PPV. Series 1 represents the best fit curve on the predicted values with R^2 value of 0.75 while series 2 is the 95% prediction curve for PPV prediction with 95% confidence interval.

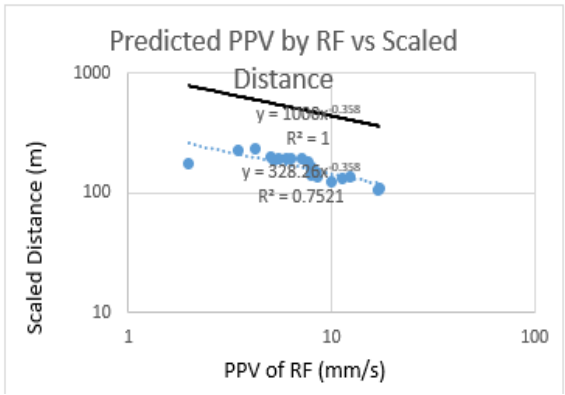

Figure 11. Graph between predicted PPV vales by random forest VS scaled distance

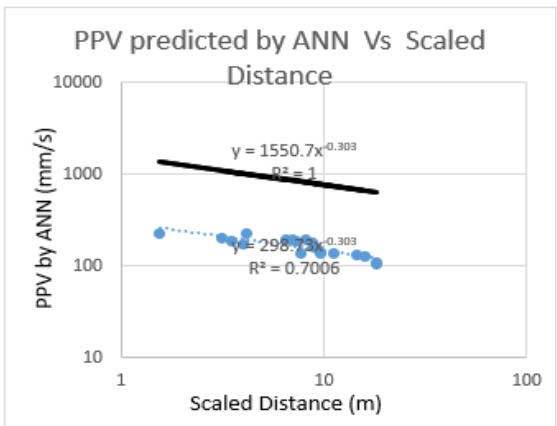

Figure 12. Graph between predicted PPV vales by ANN VS scaled distance

Figure 11 shows relation between the scaled distance and predicted PPV by random forest method. Series 1 represents the best fit curve on the predicted values with R^2 value of 0.7521 while series 2 is the 95% prediction curve for PPV prediction with 95% confidence interval.

Figure 12 shows relation between the scaled distance and predicted PPV by random forest method. Series 1 represents the best fit curve on the predicted values with R^2 value of 0.7006 while series 2 is the 95% prediction curve for PPV prediction with 95% confidence interval.

Table 10. Summary of predicted values of PPV for Mine B

Serial no	ACTUAL PPV	RANDOM FOREST	ARTIFICIAL NEURAL NETWORK
1	2.957	4.9148	5.504
2	2.797	3.0214	5.344
3	3.362	5.3198	5.909
4	6.008	9.6589	8.555
5	4.623	6.5808	7.17
6	3.238	4.1958	5.785
7	4.946	5.9038	7.493
8	5.284	6.5487	7.831
9	4.503	6.4608	7.05
10	2.664	4.6218	4.211
11	4.018	5.9758	5.565
12	3.485	5.4428	6.032
13	3.401	5.3588	4.948
14	13.49	15.0874	19.6978
15	2.232	4.1898	1.779
16	2.129	1.524	1.676
17	8.631	9.5871	14.688
18	8.106	12.0634	10.653
19	5.034	6.9918	7.581
20	2.469	4.4268	5.016
21	3.487	5.4448	6.034

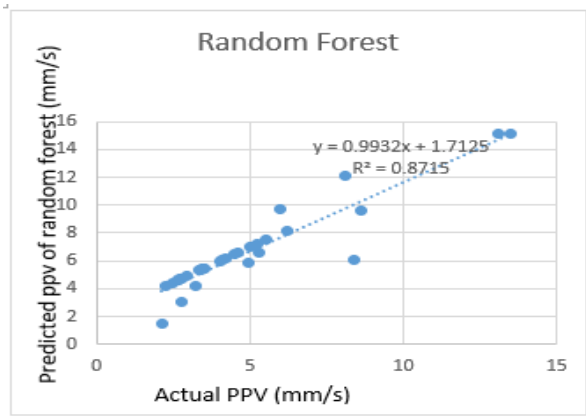

Figure 13. Graph between the comparison between the actual and predicted PPV values by Random forest

Figure 13 is the graph between actual PPV and predicted PPV values by random forest with R^2 value of 0.8715 shows they are in consonance with each other.

Figure 14 is the graph between actual PPV and predicted PPV values by Artificial Neural Network with R^2 value of 0.8136 shows they are in consonance with each other.

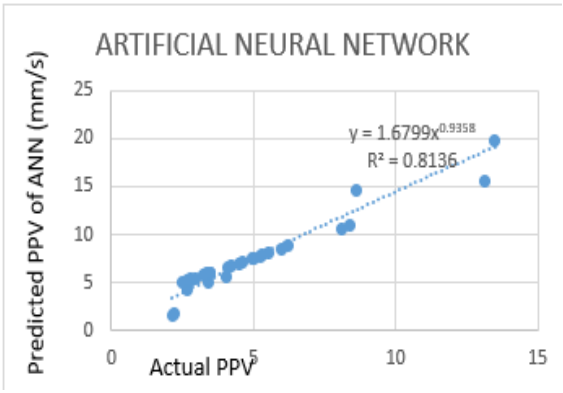

Figure 14. Graph between the comparison between the actual and predicted PPV values by Artificial neural network

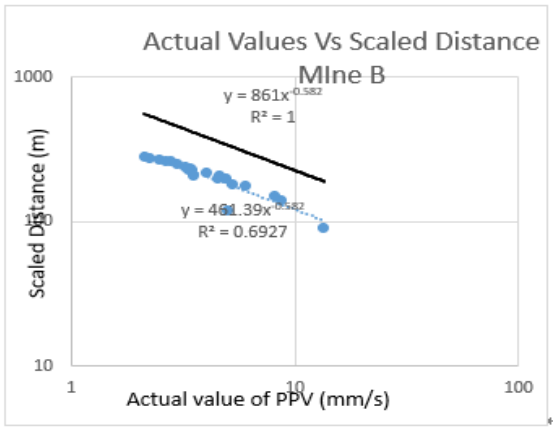

Figure 15. Graph between actual values of PPV for Mine B Vs Scaled Distance

Figure 15 shows relation between the scaled distance and actual PPV. Series 1 represents the best fit curve on the predicted values with R^2 value of 0.69 while series 2 is the 95% prediction curve for PPV prediction with 95% confidence interval.

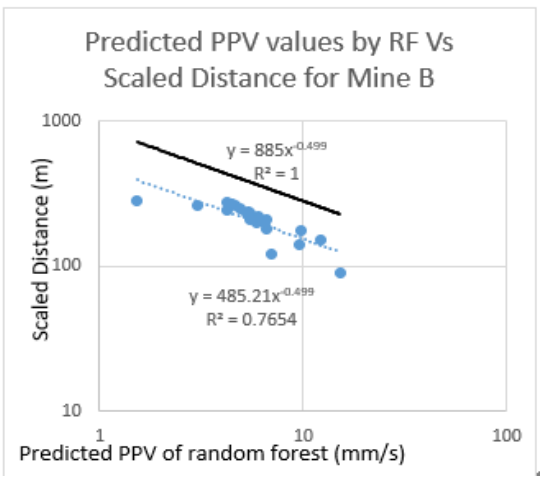

Figure 16. Graph between Predicted PPV values by Random Forest Vs scaled Distance

Figure 16 shows relation between the scaled distance and actual PPV. Series 1 represents the best fit curve on the predicted values with R^2 value of 0.7654 while series 2 is the 95% prediction curve for PPV prediction with 95% confidence interval.

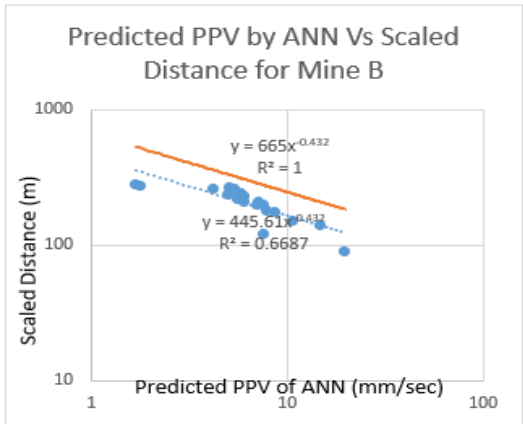

Figure 17. Graph between Predicted PPV vales by ANN VS Scaled Distance

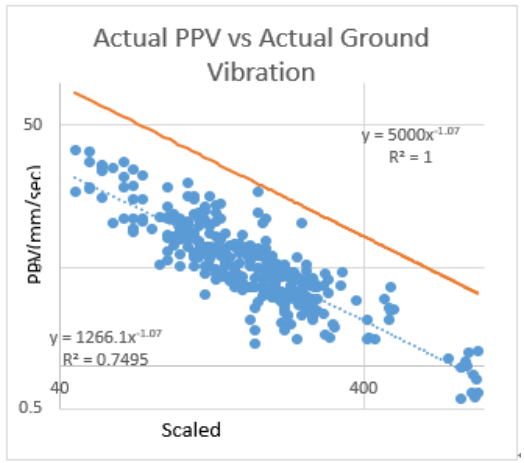

Figure 18. Graph between the Actual PPV values of all mines Vs Scaled distance

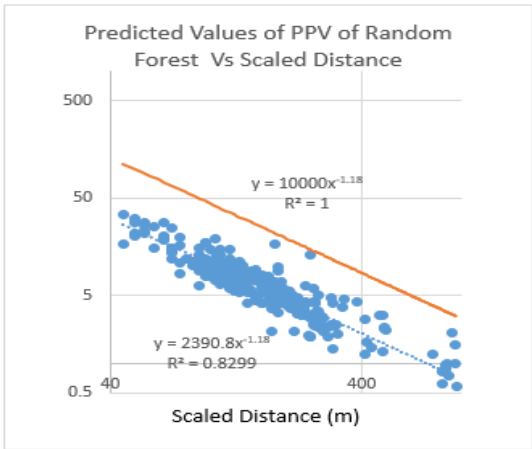

Figure 19. Graph between predicted values of PPV by random forest Vs Scaled Distance

Figure 17 shows relation between the scaled distance and actual PPV. Series 1 represents the best fit curve on the predicted values with R^2 value of 0.6687 while series 2 is the 95% prediction curve for PPV prediction with 95% confidence interval.

Figure 18 is the Graph between the Actual PPV values of all the 10 mines considered for the study and Scaled distance.

Figure 19 is the Graph between the predicted PPV values of random forest by all the 10 mines considered for the study and

Scaled distance.

5. CONCLUSION

Total of the ten open cut coal mines of Jharia coalfields were selected under this study. Total of 325 blast data was considered during the study. It has been observed that random forest method provided predicted values of PPV which was closer than the ANN predicted values to the actual values obtained at mine site. Therefore we can conclude that Random forest method is better for prediction of PPV values. Further the prediction model using random forest method at 95% confidence level has been proposed which will be very handy and useful for mining engineers of all open cut mines of Jharia Coalfield. It will be very convenient to design the blast for controlling the blast induced ground vibration for greenfield projects too.

REFERENCES

[1] Agrawal H, Mishra AK. (2018). A study on influence of density and viscosity of emulsion explosive on its detonation velocity. Model. Meas. Control C 78(3): 316-336.

[2] Khandelwal M, Singh TN. (2006). Prediction of blast induced ground vibrations and frequency in opencast mine: A neural network approach. J. Sound Vib. 289(4-5): 711-725.

[3] Singh PK, Roy MP. (2010). Damage to surface structures due to blast vibration. Int. J. Rock Mech. Min. Sci. 47(6): 949-961.

[4] Agrawal H, Mishra AK. (2018). A study on influence of density and viscosity of emulsion explosive on its detonation velocity. Model. Meas. Control C 78(3): 316-336.

[5] Khandelwal M, Singh TN. (2006). Prediction of blast induced ground vibrations and frequency in opencast mine: A neural network approach. J. Sound Vib. 289(4–5): 711-725.

[6] Singh PK, Roy MP. (2010). Damage to surface structures due to blast vibration. Int. J. Rock Mech. Min. Sci. 47(6): 949-961.

[7] Agrawal AKMH. (2018). Probabilistic analysis on scattering effect of initiation systems and concept of modified charge per delay for prediction of blast induced ground vibrations. Measurement 130: 306-317.

[8] Singh PK, Vogt W, Singh RB, Singh DP. (1996). Blasting side effects-Investigations in an opencast coal mine in India. Int. J. Surf. Min. Reclam. 10(4): 155-159.

[9] Agrawal H, Mishra AK. (2018). Evaluation of initiating system by measurement of seismic energy dissipation in surface blasting. Arab. J. Geosci. 11(13): 345.

[10] Liang Q, An Y, Zhao L, Li D, Yan L. (2011). Comparative study on calculation methods of blasting vibration velocity. Rock Mech. Rock Eng. 44(1): 93-101.

[11] Khandelwal M, Singh TN. (2009). International journal of rock mechanics & mining sciences prediction of blast-induced ground vibration using artificial neural network. Int. J. Rock Mech. Min. Sci. 46(7): 1214–1222.

[12] Tiile RN. (2016). Artificial neural network approach to predict blast-induced ground vibration, airblast and rock fragmentation. Missouri University of Science and Technology.

[13] Monjezi M, Ghafurikalajahi M, Bahrami A. (2011). Prediction of blast-induced ground vibration using artificial neural networks. Tunn. Undergr. Sp. Technol. 26(1): 46–50.

[14] Singh TN, Singh V. (2005). An intelligent approach to prediction and control ground vibration in mines. Geotech. Geol. Eng. 23(3): 249–262.

[15] Hajihassani M, Armaghani DJ, Sohaei H, Mohamad ET, Marto A. (2014). Prediction of airblast-overpressure induced by blasting using a hybrid artificial neural network and particle swarm optimization. Appl. Acoust. 80: 57-67.

[16] Ataei M, Sereshki F. (2017). Improved prediction of blast-induced vibrations in limestone mines using Genetic Algorithm. J. Min. Environ. 8(2): 291-304.

[17] Dong L, Li X, Xu M, Li Q. (2011). Comparisons of random forest and Support Vector Machine for predicting blasting vibration characteristic parameters. Procedia Eng. 26: 1772-1781.

[18] Khandelwal M, Kankar PK, Harsha SP. (2010). Evaluation and prediction of blast induced ground vibration using support vector machine. Min. Sci. Technol. 20(1): 64-70.

[19] Ranjan K, Deepankar C, Kapilesh B. (2012). Response of foundations subjected to blast loadings: State of the art review.

[20] Konya CJ, Walter EJ. (2010). Rock blasting. US Department of Transportation Federal Highway Administration.

[21] Srbulov M. (2010). Ground Waves Propagation. Ground Vibration Engineering, Springer 23-42.

[22] Ainalis D, Ducarne L, Kaufmann O, Tshibangu JP, Verlinden O, Kouroussis G. (2017). Improved blast vibration analysis using the wavelet transform. 24th International Congress on Sound and Vibration, London.

[23] Youssef AM, Pourghasemi HR, Pourtaghi ZS, Al-Katheeri MM. (2016). Landslide susceptibility mapping using random forest, boosted regression tree, classification and regression tree, and general linear models and comparison of their performance at Wadi Tayyah Basin, Asir Region, Saudi Arabia. Landslides 13(5): 839-856.

[24] Rodriguez-Galiano V, Sanchez-Castillo M, Chica-Olmo M, Chica-Rivas M. (2015). Machine learning predictive models for mineral prospectivity: An evaluation of neural networks, random forest, regression trees and support vector machines. Ore Geol. Rev. 71: 804-818.

[25] Muhammad K, Shah A. (2017). Minimising backbreak at the dewan cement limestone quarry using an artificial neural network. Arch. Min. Sci. 62(4): 795–806.

[26] Sumathi S, Paneerselvam S. (2010). Computational intelligence paradigms: theory & applications using MATLAB. CRC Press.